Online Radio Map Update based on a Marginalized Particle Gaussian Process

Zhendong Xu, Baoqi Huang, Bing Jia and Wuyungerile Li
College of Computer Science
Inner Mongolia University, Hohhot 010021 China

***Abstract*—In this paper, a novel scheme is reported to adapt radio maps to environmental dynamics in an online fashion by combining crowdsourcing and gaussian process regression (GPR). Specifically, a Marginalized Particle Gaussian Process (MPGP) is adopted to recursively fuse crowdsourced fingerprints with an existing offline radio map. The advantages of the proposed scheme lie in the efficiency and scalability in comparison with the traditional approaches. Extensive experiments are carried out in a real scenario of nearly 1000 m^2 during five months, and a comparison is made with several existing popular solutions. It is shown that the proposed scheme outperforms its counterparts in terms of both robustness and accuracy.**

I. Introduction

WiFi fingerprint-based localization is one of the most attractive and promising solution for indoor localization, and great efforts [1]–[3] have been devoted. The fingerprint-based indoor positioning system (IPS) demands a labor-intensive and time-consuming site survey in the offline phase for building a radio map. In order to reduce the offline workload, various crowdsourcing-based approaches [4]–[6] were reported to leverage daily activities of volunteers and pedestrian dead reckoning (PRD) [7]–[9] to automatically collect fingerprints; recently, the Gaussian process regression (GPR) based approaches [10] have gained much attention since the amount of RSS measurements required can be substantially decreased. However, GPR suffers from scalability on account of inverting a matrix with its order being the total number of crowdsourced fingerprints, which can be huge with time and space increasing.

The localization performance of a fingerprint-based IPS often degrades over time due to environmental dynamics. As such, a great amount of researches have been conducted to produce update-to-date radio maps. The simple solution only considers the changes of APs and replaces the outdated fingerprints in radio maps [11]–[13]. The advanced solutions incorporate new RSS measurements into existing radio maps so as to adapt to environmental dynamics. In [14], LuMA was proposed to model the problem of updating a radio map as the transfer learning problem based on dimensionality reduction, which learns a mapping from an old radio map to a new one in a low-dimensional space. In [15], a dynamic online-calibration scheme uses GPR with the log-distance path loss model to construct and calibrate radio maps, but requires re-estimating the parameters by maximizing the given likelihood function. A WiFi-based non-intrusive IPS, termed WinIPS, that enables automatic online radio map construction and adaptation was proposed in [16] for calibration-free indoor localization. Additionally, in [17], AcMu makes use of realtime RSS measurements from a static smartphone to automatically update radio maps by modeling the underlying relationship between nearby RSS measurements, which relies on the movement detection of the smartphone.

Although these efforts have made it promising to efficiently construct and update radio maps, efficiently fusing crowdsourced fingerprints is still challenging. To address this issue, this paper adopts the Marginalized Particle Gaussian Process (MPGP) to recursively adapt the radio map by using continuously crowdsourced fingerprints whose location labels are estimated based on the current radio map. The advantages of the MPGP lies in that crowdsourced fingerprints are recursively processed and their locations are not necessarily aligned with the radio map. Finally, extensive experiments are carried out in a real scenario during a five-month period of time, and it is shown that, the proposed scheme significantly outperforms several existing popular solutions in terms of both localization accuracy and robustness.

II. Online Radio Map Update

Throughout this paper, letters in bold denote matrix or vector; $\mathbb{E}(\cdot)$ and $\mathbb{V}(\cdot)$ denote the expectation and variance operators, respectively; $|\cdot|$ denotes the determinant operator; $\|\cdot\|$ denotes the Euclidean norm operator; ^{T} denotes the transpose operator; $\mathbf{I}$ is an identity matrix of proper order n.

A. GPR

Consider the following observation model

$$y = f(\mathbf{x}) + v, \tag{1}$$

where $v \sim \mathcal{N}(0, \sigma_n^2)$ represents the i.i.d. (independent, identically distributed) noise; y denotes the observation, i.e. a WiFi RSS measurement, given a particular input feature $\mathbf{x} \in \mathbb{R}^2$, i.e. 2-dimensional (2D) location coordinates.

The latent function, $f(\mathbf{x})$, can be stated as a Gaussian process (GP), namely

$$f(\mathbf{x}) \sim \mathcal{GP}(m(\mathbf{x}), k(\mathbf{x}, \mathbf{x}')), \tag{2}$$

where $m(\mathbf{x})$ and $k(\mathbf{x}, \mathbf{x}')$ are the mean function and covariance function, respectively.

According to [10], the mean function can be modelled as a quadratic polynomial of $\mathbf{x}$, namely

$$m(\mathbf{x}) = \mathbf{x}^T \mathbf{A} \mathbf{x} + \mathbf{b}^T \mathbf{x} + c, \tag{3}$$

where $\mathbf{A} = [\mathbf{A}_{11}, \mathbf{A}_{12}; \mathbf{A}_{12}, \mathbf{A}_{22}]$, $\mathbf{b} = [\mathbf{b}_1; \mathbf{b}_2]$ and c are coefficients, and the covariance function can be modelled using the squared exponential kernel function, namely

$$k(\mathbf{x}, \mathbf{x}') = \sigma_f^2 \exp\left(-\frac{\|\mathbf{x} - \mathbf{x}'\|}{2l^2}\right), \tag{4}$$

where σ_f^2 and l denote the signal variance and scale parameter.

Given n location labels $\mathbf{X} = [\ \mathbf{x}_1 \ \cdots \ \mathbf{x}_n\ ]$ with $\mathbf{x}_i \in \mathbb{R}^2, i = 1, \cdots, n$, the corresponding observations, i.e. RSS measurements from an arbitrary access point (AP), are defined to be $\mathbf{y} = [\ y_1 \ \cdots \ y_n\ ]^T$. It is evident that

$$\mathbf{y}|\mathbf{X} \sim \mathcal{N}(\mathbf{m}(\mathbf{X}), \mathbf{K}(\mathbf{X}, \mathbf{X}) + \sigma_n^2 \mathbf{I}), \tag{5}$$

where the element at the i-th row and j-th column of the $n \times n$ matrix $\mathbf{K}(\mathbf{X}, \mathbf{X}')$ equals to $k(\mathbf{x}_i, \mathbf{x}'_j)$ with $\mathbf{x}_i$ being the i-th column of $\mathbf{X}$ and $\mathbf{x}'_j$ being the j-th column of $\mathbf{X}'$.

Let the unknown parameters form a vector $\theta = [\mathbf{A}_{11}, \mathbf{A}_{22}, \mathbf{A}_{12}, \mathbf{b}_1, \mathbf{b}_2, c, \sigma_n, \sigma_f, l]^T$, also termed hyperparameters of the GP. Since any finite number of collections sampled from a GP follow a joint Gaussian distribution [18], the log likelihood of the observations in $\mathbf{y}$ is given by

$$\begin{aligned}\log \mathcal{L}(\mathbf{y}; \mathbf{X}, \theta) = &-\frac{n}{2}\log 2\pi - \frac{1}{2}\log|(\mathbf{K}(\mathbf{X}, \mathbf{X}) + \sigma_n^2 \mathbf{I})| \\ &-\frac{1}{2}(\mathbf{y} - \mathbf{m}(\mathbf{X}))^T(\mathbf{K}(\mathbf{X}, \mathbf{X}) + \sigma_n^2 \mathbf{I})^{-1}(\mathbf{y} - \mathbf{m}(\mathbf{X})).\end{aligned} \tag{6}$$

The hyperparameters θ can be estimated by maximizing (6), such that the mean and variance of RSS measurements at any location, say $\mathbf{x}_*$, can be predicted through GPR. As such, the radio map can be interpolated with RSS measurements at only a relatively small number of locations.

B. State Space Model

In order to estimate both the hyperparameters θ and hidden function values f in an online fashion, we define a new state space model in what follows.

Firstly, to filter the hidden static hyperparameters, an artificial evolution is added using kernel smoothing which guarantees the estimation convergence [19]

$$\theta_t = b\theta_{t-1} + (1 - b)\bar{\theta}_{t-1} + s_{t-1}, \tag{7}$$

where $b = (3\delta - 1)/(2\delta)$, δ is a discount factor which is typically around $0.95 - 0.99$, $\bar{\theta}_{t-1}$ is the Monte Carlo mean of θ at $t-1$, and $s_{t-1} \sim \mathcal{N}(0, r^2\Sigma_{t-1})$, $r^2 = 1 - b^2$, Σ_{t-1} is the Monte Carlo variance matrix of θ at $t-1$.

Secondly, to explore the relation between the crowdsourcing RSS measurements at $t-1$ and t, define $\mathbf{X}_t^c = [\mathbf{X}_t, \mathbf{X}_*]$ and $\mathbf{f}_t^c = \mathbf{f}(\mathbf{X}_t^c)$, where $\mathbf{X}_t$ is the location labels of the crowdsourcing RSS measurements at t and $\mathbf{X}_*$ denotes the locations of the fingerprints in the radio map. Since $f(\mathbf{x}) \sim GP(m(\mathbf{x}), k(\mathbf{x}, \mathbf{x}'))$, then the prior distribution $p(\mathbf{f}_t^c, \mathbf{f}_{t-1}^c|\mathbf{X}_{t-1}^c, \mathbf{X}_t^c, \theta_t)$ is jointly Gaussian.

Then, according to the conditional property of the Gaussian distribution, we can obtain $p(\mathbf{f}_t^c|\mathbf{f}_{t-1}^c, \mathbf{X}_{t-1}^c, \mathbf{X}_t^c, \theta_t)$ is Gaussian with

$$\mathcal{N}(\mathbf{G}(\theta_t)\mathbf{f}_{t-1}^c + \mathbf{F}(\theta_t), \mathbf{V}(\theta_t)), \tag{8}$$

where

$$\begin{aligned}\mathbf{G}(\theta_t) &= \mathbf{K}_{\theta_t}(\mathbf{X}_t^c, \mathbf{X}_{t-1}^c)\mathbf{K}_{\theta_t}^{-1}(\mathbf{X}_{t-1}^c, \mathbf{X}_{t-1}^c), &(9)\\ \mathbf{F}(\theta_t) &= \mathbf{m}_{\theta_t}(\mathbf{X}_t^c) - \mathbf{G}(\theta_t)\mathbf{m}_{\theta_t}(\mathbf{X}_{t-1}^c), &(10)\\ \mathbf{V}(\theta_t) &= \mathbf{K}_{\theta_t}(\mathbf{X}_t^c, \mathbf{X}_t^c) - \mathbf{G}(\theta_t)\mathbf{K}_{\theta_t}(\mathbf{X}_t^c, \mathbf{X}_{t-1}^c)^T. &(11)\end{aligned}$$

Hence, the following state equation can be derived by transforming the conditional density in (8) into a linear equation of the function value with additive Gaussian noises $\mathbf{v}_t^f \sim \mathcal{N}(\mathbf{0}, \mathbf{V}(\theta_t))$:

$$\mathbf{f}_t^c = \mathbf{G}(\theta_t)\mathbf{f}_{t-1}^c + \mathbf{F}(\theta_t) + \mathbf{v}_t^f. \tag{12}$$

Moreover, the observation equation could be directly obtained from the RSS measurements at t

$$\mathbf{y}_t = \mathbf{H}_t\mathbf{f}_t^c + \mathbf{v}_t^y, \tag{13}$$

where $\mathbf{H}_t = [\mathbf{I}, \mathbf{0}]$ makes $\mathbf{H}_t\mathbf{f}_t^c = \mathbf{f}(\mathbf{X}_t)$, the order of $\mathbf{I}$ is n_t representing the number of noisy location labels in $\mathbf{X}_t$, and $\mathbf{v}_t^y$ is additive Gaussian noise satisfying $\mathcal{N}(\mathbf{0}, \sigma_n^2\mathbf{I})$.

The state space model is specified by (7), (12) and (13).

C. Online Updating with MPGP

In contrast to the traditional GPR inferring hidden function values in an offline manner, we adopt the online filtering framework proposed in [19] to simultaneously learn the hyperparameters and estimate hidden function values, i.e. $p(\mathbf{f}_t^c, \theta_{1:t}|\mathbf{X}_{1:t}, \mathbf{X}_*, \mathbf{y}_{1:t})$, by combining Kalman filter into particle filter.

The whole algorithm is summarized as follows:

1) For each of the particle, say the i-th one with $i = 1, 2, \cdots, N$
   - Drawing $\theta_t^i \sim p(\theta_t|\tilde{\theta}_{t-1}^i)$ according to (7);
   - Using θ_t^i to compute $k(\mathbf{x}, \mathbf{x}')$, $\mathbf{G}(\theta_t^i), \mathbf{F}(\theta_t^i), \mathbf{V}(\theta_t^i)$ and $\sigma_n^2\mathbf{I}$ in (9), (10), (11) and (13);
   - Kalman predicting, namely computing $\tilde{\mathbf{f}}_{t|t-1}^{c,i}, \tilde{\mathbf{P}}_{t|t-1}^{c,i}$ with $\tilde{\mathbf{f}}_{t-1|t-1}^{c,i}, \tilde{\mathbf{P}}_{t-1|t-1}^{c,i}$ by

$$\begin{aligned}\mathbf{f}_{t|t-1}^c &= \mathbf{G}(\theta_t)\mathbf{f}_{t-1|t-1}^c + \mathbf{F}(\theta_t), &(14)\\ \mathbf{P}_{t|t-1}^c &= \mathbf{G}(\theta_t)\mathbf{P}_{t-1|t-1}^c\mathbf{G}(\theta_t)^T + \mathbf{V}(\theta_t). &(15)\end{aligned}$$

   - Kalman updating, namely computing $\tilde{\mathbf{f}}_{t|t}^{c,i}, \tilde{\mathbf{P}}_{t|t}^{c,i}$ with $\tilde{\mathbf{f}}_{t|t-1}^{c,i}, \tilde{\mathbf{P}}_{t|t-1}^{c,i}$ by

$$\begin{aligned}\mathbf{\Gamma}_t &= \mathbf{P}_{t|t-1}^c\mathbf{H}_t^T(\mathbf{H}_t\mathbf{P}_{t|t-1}^c\mathbf{H}_t^T + \sigma_n^2\mathbf{I})^{-1}, &(16)\\ \mathbf{f}_{t|t}^c &= \mathbf{f}_{t|t-1}^c + \mathbf{\Gamma}_t(\mathbf{y}_t - \mathbf{H}_t\mathbf{f}_{t|t-1}^c), &(17)\\ \mathbf{P}_{t|t}^c &= \mathbf{P}_{t|t-1}^c - \mathbf{\Gamma}_t\mathbf{H}_t\mathbf{P}_{t|t-1}^c. &(18)\end{aligned}$$

     where $\mathbf{\Gamma}_t$ is the Kalman gain.
   - Weighting, namely computing the importance weight $\bar{w}_t^i$ with $\tilde{\mathbf{f}}_{t|t-1}^{c,i}, \tilde{\mathbf{P}}_{t|t-1}^{c,i}, \sigma_n^2\mathbf{I}$ by;

$$\begin{aligned}\bar{w}_t^i = &\ w_{t-1}^i \times p(\mathbf{f}_{t|t}^c|\theta_{1:t}, \mathbf{X}_{1:t}, \mathbf{X}_*, \mathbf{y}_{1:t})p(\theta_t|\theta_{t-1}) \\ &\times\mathcal{N}(\mathbf{H}_t\mathbf{f}_{t|t-1}^c, \mathbf{H}_t\mathbf{P}_{t|t-1}^c\mathbf{H}_t^T + \sigma_n^2\mathbf{I}),\end{aligned} \tag{19}$$

     where $p(\theta_t|\theta_{t-1})$ and $p(\mathbf{f}_{t|t}^c|\theta_{1:t}, \mathbf{X}_{1:t}, \mathbf{X}_*, \mathbf{y}_{1:t})$ can be computed using (7) and (12) respectively.

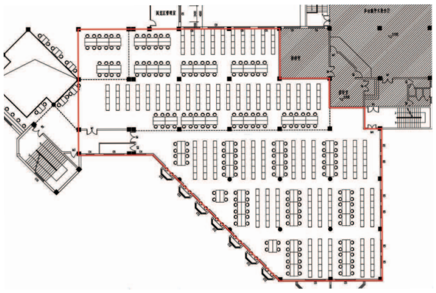

Fig. 1. The floor plan of experimental areas.

2) Normalizing the weight $w_t^i = \bar{w}_t^i / \Sigma_{j=1}^N \bar{w}_t^j$;
3) Hyperparameter and hidden function value estimation:

$$\begin{aligned}\hat{\theta}_t &= \Sigma_{i=1}^N w_t^i \tilde{\theta}_t^i, \\ \hat{\mathbf{f}}_{t|t}^c &= \Sigma_{i=1}^N w_t^i \tilde{\mathbf{f}}_{t|t}^{c,i}, \\ \hat{\mathbf{P}}_{t|t}^c &= \Sigma_{i=1}^N w_t^i (\tilde{\mathbf{P}}_{t|t}^{c,i} + (\tilde{\mathbf{f}}_{t|t}^{c,i} - \hat{\mathbf{f}}_{t|t}^c)(\tilde{\mathbf{f}}_{t|t}^{c,i} - \hat{\mathbf{f}}_{t|t}^c)^T),\end{aligned}$$

implying that

$$\begin{aligned}\hat{\mathbf{f}}_{t|t}^* &= \mathbf{H}_t^* \hat{\mathbf{f}}_{t|t}^c, \\ \hat{\mathbf{P}}_{t|t}^* &= \mathbf{H}_t^* \hat{\mathbf{P}}_{t|t}^c (\mathbf{H}_t^*)^T,\end{aligned}$$

where $\mathbf{H}_t^* = [\ \mathbf{0} \quad \mathbf{I}_m\ ]$ is an index matrix to obtain the function value estimation at $\mathbf{X}_*$;
4) Resampling: for $i = 1, 2, \cdots, N$, resample $\theta_t^i, \mathbf{f}_{t|t}^{c,i}, \mathbf{P}_{t|t}^{c,i}$ with respect to the importance weight w_t^i to obtain $\tilde{\theta}_t^i, \tilde{\mathbf{f}}_{t|t}^{c,i}, \tilde{\mathbf{P}}_{t|t}^{c,i}$ for the next step;
5) Increasing t by 1 and repeat Step 1).

At each iteration, the MPGP uses a small training subset to estimate $\mathbf{f}(\mathbf{X}_*)$ by Kalman filters, and learn hyperparameters online by weighted particles.

In order to launch the aforementioned algorithm at $t = 1$, we need to initialize the values of $\tilde{\theta}_0^i, \tilde{\mathbf{f}}_{0|0}^{c,i}, \tilde{\mathbf{P}}_{0|0}^{c,i}$ with $i = 1, 2, \cdots, N$. Therefore, the first set of crowdsourced RSS measurements is utilized to produce the initial estimate of the hyperparameters θ_0 as well as the mean $\mathbb{E}(\mathbf{f}_0^c)$ and variance $\mathbb{V}(\mathbf{f}_0^c)$ at $\mathbf{U}_0^c$. Then, let $\tilde{\theta}_0^i = \theta_0$, $\tilde{\mathbf{P}}_{0|0}^{c,i} = \mathbb{V}(\mathbf{f}_0^c)$, and draw $\tilde{\mathbf{f}}_{0|0}^{c,i}$ from $\mathcal{N}(\mathbb{E}(\mathbf{f}_0^c), \mathbb{V}(\mathbf{f}_0^c))$.

III. Performance Evaluation

In this section, extensive experiments are conducted to thoroughly evaluate the performance of the proposed method.

A. Experimental Setup

In the experiments, realistic RSS measurements are collected in a large open space, i.e. the Reading Room on the 3rs floor of the library building at Inner Mongolia University, which covers a total area of nearly 1000 m^2 and includes 57 bookracks with the height of around 2 m as well as a number of big and long desks and chairs, as shown in Fig. 1. The space is divided by a regular lattice with the interval of 1 m and thus totally includes 938 lattice points as reference points.

The experiments lasted five months. Specifically, 10 sets of RSS measurements were collected with different intervals (e.g. one day, one week, one month, two months, and etc.) at different times (e.g. weekday, weekend, holiday, daytime and evening) to fully take into consideration environmental dynamics. At each time, a student arbitrarily traversed the Reading Room as usual to produce training RSS measurements with a smartphone (HUAWEI P7) held in front of his chest, and additionally, walked 7 trajectories between 20 m and 30 m to produce testing RSS measurements by accurately labelling their locations. Note that an Android APP was developed by us to facilitate the collection of RSS measurements.

In the experiments, 22 APs are detected by the smartphone. A coarse-grained radio map is initially constructed in the offline phase by using the training RSS measurements (whose accurate location labels are available) collected in the first time based on the GPR approach; then, according to the chronological order, the training RSS measurements collected in the other 9 times are employed to update or produce the radio map in 9 rounds by using different methods; the corresponding testing RSS measurements are used for localization by using the weighted k nearest neighbor (WKNN) method with $k = 6$.

Several popular approaches are implemented for comparison. Two GPR based approaches [15] with zero mean and polynomial mean function like (3) respectively, i.e. Zero Mean GPR (ZM GPR) and GPR, are taken into account. These two approaches just abandon existing radio maps and generate brandnew radio maps as long as new training RSS measurements are available, namely that new RSS measurements are not fused with existing radio maps. Since AcMu in [17] mainly relies on the fusion method, i.e. the partial least squares regression (PLSR) method, and requests realtime RSS measurements at certain reference points with static smartphones, which does not match with the the scenario considered in our experiments, a PLSR based radio map updating method similar to AcMu is implemented with 200 points randomly selected as pseudo reference points by averaging the training RSS measurements at their vicinities (i.e. within 2 m). In order to provide as good emulation as possible, the training RSS measurements in the current round and past one round are used for averaging.

The experiments are carried out in Matlab. The space is divided into 10 subregion with the area of around 100 m^2, and in each subregion, MPGP is implemented with the particle number of 500.

B. Results

In order to validate the effectiveness of the proposed scheme, comparisons with other three approaches are made in terms of both RSS prediction and localization.

TABLE I
Comparison of the mean and standard deviation of the RSS prediction errors produced by different approaches.

Method	RSS Prediction Error (dBm)	
	Average	Standard deviation
MPGP	6.94	1.99
PLSR	14.08	3.87
ZM GPR	28.67	5.80
GPR	11.31	2.77

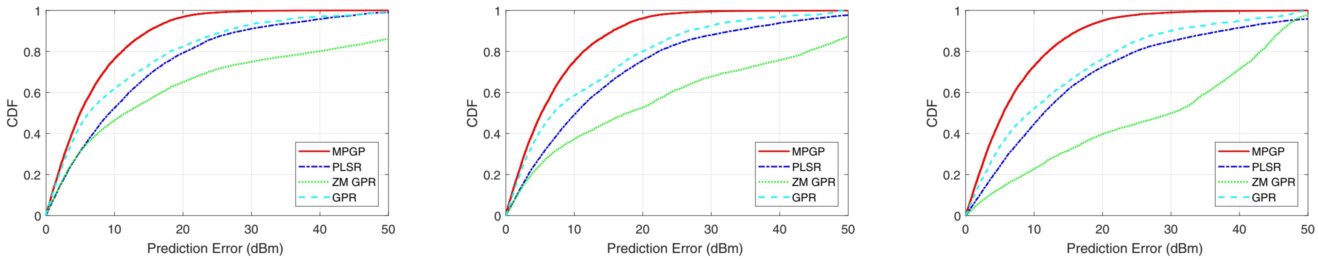

(a) After one month (b) After two months (c) After five months

Fig. 2. Comparison of the RSS prediction errors with respect to different times.

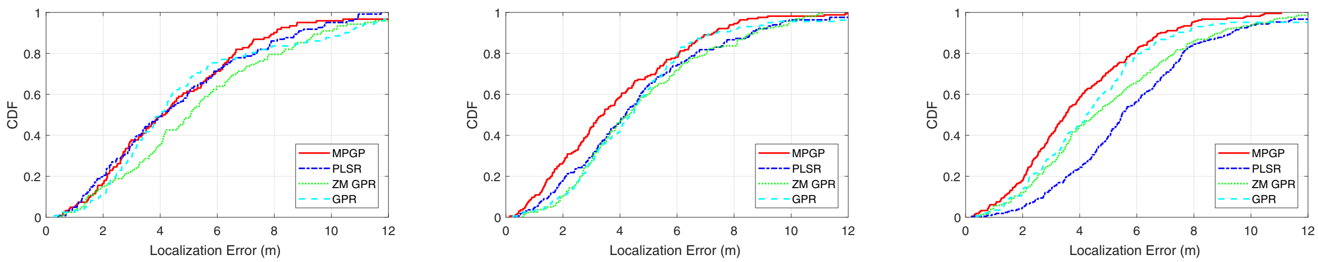

(a) After one month (b) After two months (c) After five months

Fig. 3. Comparison of localization errors produced by different approaches at different times.

In the first place, the RSS prediction performance is e-valuated. Define the RSS prediction error to be the absolute difference between that predicted by one approach and ground truth. Note that, since acquiring the ground truth of the expected RSS measurement at any reference point is hard or even impossible, it is approximately evaluated by averaging the RSS measurements within 2 m of this reference point.

The means and standard deviations of the RSS prediction errors are listed in Table I, and the cumulative density function (CDF) of the RSS prediction error with respect to one month (i.e. NO. 2 round), two months (i.e. NO. 4 round) and five months (i.e. NO. 9 round) are illustrated in Fig. 2. As can be seen, the RSS prediction errors are less than 7 dBm for the proposed scheme, but doubled or even worse for the other three counterparts. More importantly, the standard deviations associated with the proposed scheme are also much less than those of the counterparts. Therefore, it can be concluded that the proposed scheme not only achieves relatively good RSS prediction performance, but also provides robust prediction, in comparison with the other approaches.

In the second place, the localization performance of different approaches is evaluated. The localization errors produced by four approaches with respect to 9 rounds of radio map updating are plotted in Fig. 4, and their CDFs at different times are illustrated in Fig. 3. As can be seen, the average localization error of the proposed scheme gradually decreases from 4.98 m to 3.93 m, whereas those of the other three approaches mainly fluctuate between 4.5 m and 6 m. Specifically, ZM GPR derives worst performance, PLSR appears to degrade with time elapsing, and GPR suffers from high fluctuation.

In summary, the extensive experiments validate the superiority and robustness of the proposed scheme.

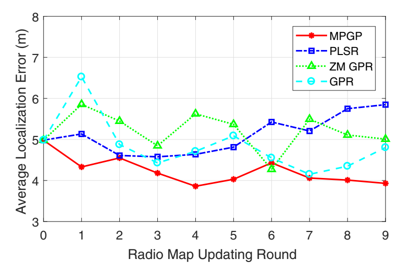

Fig. 4. Comparison of localization errors produced by different approaches with respect to 9 rounds.

IV. Conclusion

This paper proposed to recursively update radio maps using crowdsourced fingerprints in an online fashion. To be specific, MPGP was adopted to fuse crowdsourced fingerprints with existing radio map without the alignment of location labels. Extensive experiments were conducted, and a thorough comparison reveals that the proposed scheme outperforms the other three approaches in the literature in terms of both localization accuracy and robustness.

V. Acknowledgement

Thanks to the National Natural Science Foundation of China (Grants No. 41871363, 6146103741761086 and 61761035), the Natural Science Foundation of Inner Mongolia Autonomous Region of China (Grant No. 2017JQ09), and the Grassland Elite Project of the Inner Mongolia Autonomous Region (Grant No. CYYC5016).

REFERENCES

[1] H. Zou, B. Huang, X. Lu, H. Jiang, and L. Xie, "A robust indoor positioning system based on the procrustes analysis and weighted extreme learning machine," *IEEE Trans. Wireless Commun.*, vol. 15, no. 2, pp. 1252–1266, 2016.

[2] B. Jia, B. Huang, H. Gao, and W. Li, "Dimension reduction in radio maps based on the supervised kernel principal component analysis," *Soft Computing*, vol. 22, no. 23, pp. 7697–7703, 2018.

[3] B. Huang, M. Liu, Z. Xu, and B. Jia, "On the performance analysis of wifi based localization," in *2018 IEEE International Conference on Acoustics, Speech and Signal Processing (ICASSP)*. IEEE, 2018, pp. 4369–4373.

[4] B. Ferris, D. Fox, and N. D. Lawrence, "Wifi-slam using gaussian process latent variable models." in *IJCAI*, vol. 7, no. 1, 2007, pp. 2480–2485.

[5] A. Rai, K. K. Chintalapudi, V. N. Padmanabhan, and R. Sen, "Zee: zero-effort crowdsourcing for indoor localization," in *Mobicom '12*. ACM, pp. 293–304.

[6] Z. Yang, C. Wu, and Y. Liu, "Locating in fingerprint space: wireless indoor localization with little human intervention," in *Proceedings of the 18th annual international conference on Mobile computing and networking*. ACM, 2012, pp. 269–280.

[7] X. Yang and B. Huang, "An accurate step detection algorithm using unconstrained smartphones," in *The 27th Chinese Control and Decision Conference (2015 CCDC)*. IEEE, 2015, pp. 5682–5687.

[8] X. Kang, B. Huang, and G. Qi, "A novel walking detection and step counting algorithm using unconstrained smartphones," *Sensors*, vol. 18, no. 1, p. 297, 2018.

[9] B. Huang, G. Qi, X. Yang, L. Zhao, and H. Zou, "Exploiting cyclic features of walking for pedestrian dead reckoning with unconstrained smartphones," in *Ubicomp '16*. ACM, 2016, pp. 374–385.

[10] H. Zhao, B. Huang, and B. Jia, "Applying kriging interpolation for wifi fingerprinting based indoor positioning systems," in *WCNC '16*. IEEE, 2016, pp. 1–6.

[11] T. Gallagher, B. Li, A. G. Dempster, and C. Rizos, "Database updating through user feedback in fingerprint-based wi-fi location systems," in *Ubiquitous Positioning Indoor Navigation and Location Based Service (UPINLBS), 2010*. IEEE, 2010, pp. 1–8.

[12] J.-S. Lim, W.-H. Jang, G.-W. Yoon, and D.-S. Han, "Radio map update automation for wifi positioning systems," *IEEE Communications Letters*, vol. 17, no. 4, pp. 693–696, 2013.

[13] S. He, W. Lin, and S.-H. G. Chan, "Indoor localization and automatic fingerprint update with altered ap signals," *IEEE Transactions on Mobile Computing*, vol. 16, no. 7, pp. 1897–1910, 2017.

[14] Z. Sun, Y. Chen, J. Qi, and J. Liu, "Adaptive localization through transfer learning in indoor wi-fi environment," in *Machine Learning and Applications, 2008. ICMLA'08. Seventh International Conference on*. IEEE, 2008, pp. 331–336.

[15] M. M. Atia, A. Noureldin, and M. J. Korenberg, "Dynamic online-calibrated radio maps for indoor positioning in wireless local area networks," *IEEE Transactions on Mobile Computing*, vol. 12, no. 9, pp. 1774–1787, 2013.

[16] H. Zou, M. Jin, H. Jiang, L. Xie, and C. J. Spanos, "Winips: Wifi-based non-intrusive indoor positioning system with online radio map construction and adaptation," *IEEE Transactions on Wireless Communications*, vol. 16, no. 12, pp. 8118–8130, 2017.

[17] C. Wu, Z. Yang, and C. Xiao, "Automatic radio map adaptation for indoor localization using smartphones," *IEEE Transactions on Mobile Computing*, vol. 17, no. 3, pp. 517–528, 2018.

[18] C. E. Rasmussen, "Gaussian processes for machine learning," 2006.

[19] Y. Wang and B. Chaib-draa, "A marginalized particle gaussian process regression," in *Advances in Neural Information Processing Systems 25*, F. Pereira, C. J. C. Burges, L. Bottou, and K. Q. Weinberger, Eds. Curran Associates, Inc., 2012, pp. 1187–1195. [Online]. Available: http://papers.nips.cc/paper/4850-a-marginalized-particle-gaussian-process-regression.pdf